

### 3.1.2.5 ACS

An Annular Coupled Structure (ACS) [1] linac has been developed for the 190.8 MeV to 400 MeV part. This consists of 46 normal conducting cavities and the total length is 108.3 m. The ACS linac is a kind of coupled cavity linac and it is operated in a  $\pi/2$  standing wave mode. In the cavity, acceleration cells and annular coupling cells are alternately located with cylindrical symmetry. The main parameter is shown in Table 2.1.4.1.1. Also, two short buncher modules in MEBT2 part have the same structure.

The operating frequency of the ACS linac is 972 MHz. Before the start of this joint project, the ACS was investigated and successfully improved during the KEK Japan Hadron Project (JHP) research [2-6]. Then, the whole system was developed for 1296 MHz and the fabrication program was established through the experimental proof. The particulars of the operating frequency change are described in the reference [7]. If we scale up the design for the new frequency, the cavity dimensions are four over three times as large as that for the JHP-ACS. The results increase the difficulty of precision machining and brazing in the fabrication. In addition, the cooling of the cavities is more important because of the large duty factor operation in the future.

In the development of the new frequency ACS linac, therefore, we have taken into account the design that the appropriate RF property coexists with the compact cavity dimensions for mass-production. The JHP-ACS design has been treated as a reference. As a result of the new development, the ACS cavity has the same transverse dimensions as the JHP-ACS. In order to simplify the frequency measurement including tuning procedure and farther reduce the accelerating field perturbation, the mirror symmetrizing of coupling slots faced in the accelerating cell is adopted. The improved design keeping the structure advantage has been confirmed through numerical simulations and cold model tests.

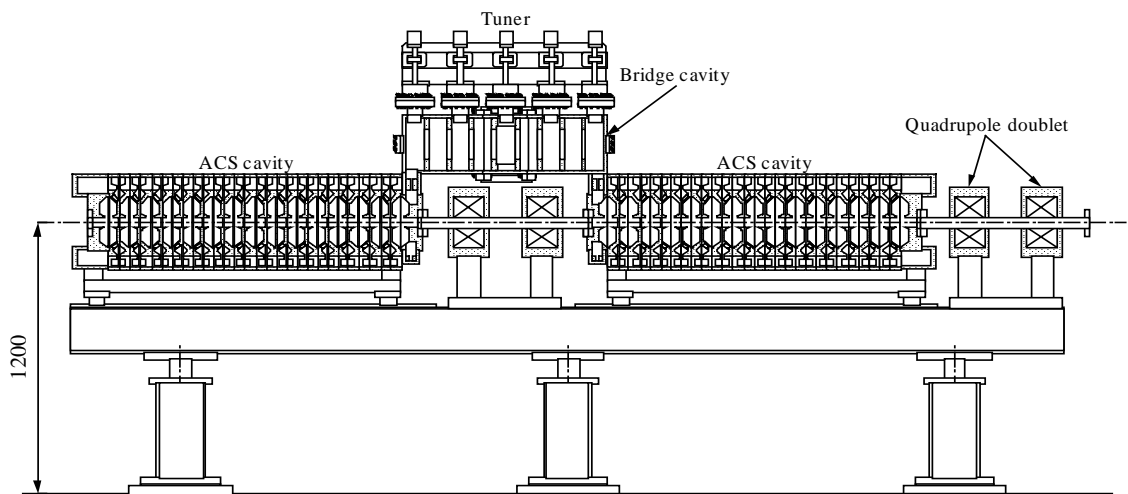


Figure 3.1.2.5.1. Layout of ACS acceleration module.

### 3.1.2.5.1 Cavity Fabrication

The ACS linac will be placed on the beam line as a series of 23 modules. Each module consists of two ACS cavities, one bridge cavity and two quadruple doublets. The design layout is shown in Figure 3.1.2.5.1. The cavities are fabricated by stacking and brazing Oxygen -Free-Copper (OFC) segments. The ACS cavities are formed with two end segments and many intermediate half-cell segments with a half-accelerating cell and a half-coupling cell. The intermediate half-cell segment is shown in Figure 3.1.2.5.2. Water cooling channels and vacuum pumping ports are machined into the half-cell segments. The bridge cavity consists of five exciting cells equipped with a movable tuner and four coupling cells.

The fabrication scheme was established during the JHP-ACS development. The ACS cavities and bridge cavity are machined with a super-precision lathe and a milling machine. The process is divided into several steps. The OFC ingot is forged into the required cell profile in a material factory. The forged OFC block is rough-machined to the designed configuration with a margin. Then the machining of coupling slots are finished with a milling machine. After this process, all blocks are annealed in order to remove the residual stresses that would otherwise be released during finish-machining. This process is important for obtaining the accurate finish-machining, and it is also reconfirmed by brazing examination. The annealed block is finish-machined including the water-cooling channel and pumping ports. Before the brazing process, the resonant frequency of the half accelerating cell and half coupling cell will be tuned within 100 kHz of the designed value. If the measured frequency

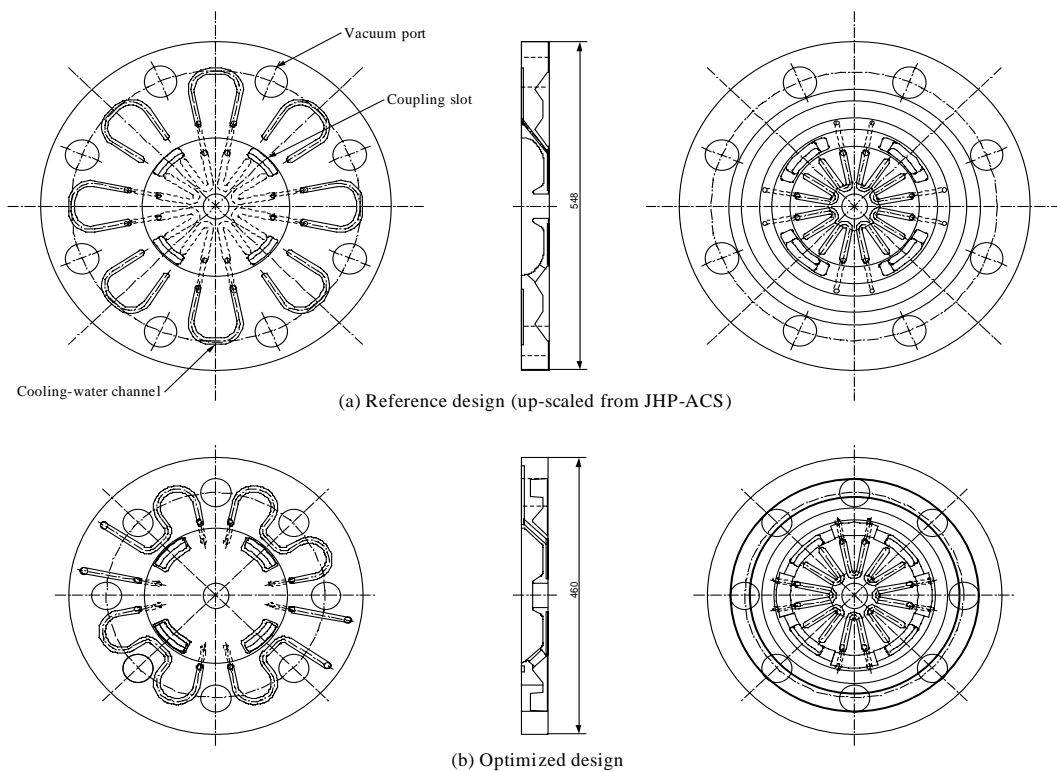


Figure 3.1.2.5.2 ACS intermediate cell configurations.

is over than the acceptable range, the tuning bump attached in each cell will be machined. The brazing process is divided into three steps. The bridge cavity is brazed with Au-alloy at the first and second step. The ACS cavity and the bridge cavity are brazed with Ag-alloy at the final step. We carried out the brazing examination with some up-scaled JHP-ACS reference models and validated that complete annealing process after rough-machining and careful brazing are important. For the optimized ACS design, each process in the fabrication will make more certain results because of large reduction of the cavity diameter.

#### 3.1.2.5.2 Cavity Design

The essential design points proved in the JHP-ACS research are the following:

- a) Four coupling slots style, to avoid mode mixing problem with high order modes in coupling cell and to provide more clean axisymmetric accelerating field distribution,
- b) Coupling slots with taper edge, to increase the coupling coefficient and to combine it with structure mechanical strength requirements,
- c) Elaborated water circuit scheme for uniform and effective structure cooling,
- d) Multi-cell bridge cavity with movable tuners, to combine two ACS cavities in one Klystron module, avoiding the mode mixing problem and providing possibility of fast and precise frequency tuning.

The configuration of accelerating cells was optimized to have high shunt impedance value in total energy range, together with reasonable maximal electric field value and careful matching with coupling cells. In addition, the mirror symmetrizing of the coupling slots faced in the accelerating cell is adopted for simplifying the frequency measurement. The details of optimization are described in the reference [8]. The maximal electric field value at the drift tube nose is varied in the maximal field  $E_{\text{smax}}/E_k$  less than 1.0 as reliable and proof value to ensure the stable operation. Although it is possible to increase  $E_{\text{smax}}/E_k$  up to 1.3 with the total shunt impedance improvement of 4 %, the price is not sufficient for the risk of breakdowns and beam pulse losses in the injecting part of this linac system.

The peripheral part of accelerating cell modified to conical style, instead of initially toroidal, to simplify matching with coupling cell and coupling slots treatment. Although the accelerating cell with a conical part has 3 % lower shunt impedance, the coupling slot rounding provides more uniform RF current distribution and finally results in higher impedance value and a small coupling coefficient increasing. The values of dimensions are fixed in the condition that the difference of total shunt impedance is minimal between the constant dimensions and completely variable (from tank to tank, to reach maximal possible impedance value) options. With the fixed dimension, the deviation from maximal possible impedance is less than 2 %.

The most serious revision has been performed for coupling cell design. The shape

was changed to reduce the outer diameter and improve the frequency separation between high order modes. The coupling cell has the same dimension for all ACS tanks. The pumping ports are shifted inside coupling cells, penetrating from cell to cell through ACS tank. The possible increasing of neighbor coupling coefficients was examined and founded in tolerable limits. The electric coupling through pumping ports just compensates with the initial magnetic coupling from coupling slots.

With mirror symmetry position of coupling slots in accelerating cells and pumping ports inside coupling cells, there is no practical distortion of the ACS dispersion curve. The neighbor coupling coefficients slightly improved (to 6% for 190.8 MeV and 5.5% for 400 MeV). It is more important for the structure parameters stability. All effects of the field generations in coupling cells; transient effects, beam loading, accelerating cells detuning and multipactoring discharge were examined during the optimization and founded inside safe limits [8].

The bridge cavity connects two ACS cavities with the appropriate beam drift length in the module and divides RF power fed through a waveguide. It consists of five exciting cells and four coupling cells (three and two cells for buncher modules in MEBT2, respectively) and the center exciting cell is equipped with a waveguide type coupler. The cell number was selected to provide the appropriate coupling with ACS cavities and ensure safe frequency separations between high order modes. The top of the exciting cells is equipped with movable frequency tuners of a plunger insertion type for fast tuning. Coupling section between

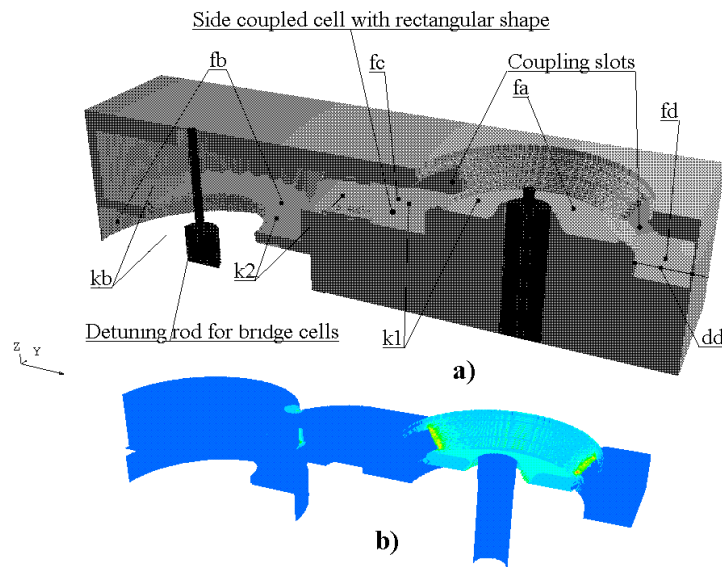


Figure 3.1.2.5.3 Coupling section between a bridge cavity and an ACS end cell with a side-coupled cell, (a) detuning rods for frequency determination and notation for coupled circuit analysis and (b) RF losses density distribution.

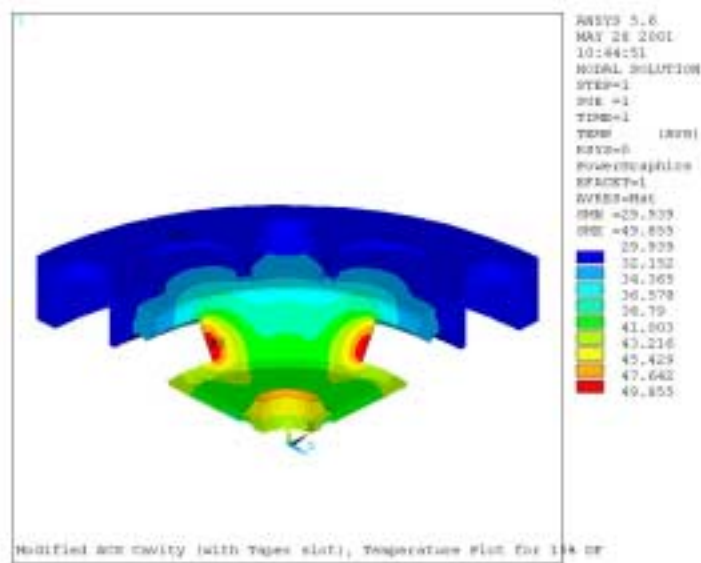


Figure 3.1.2.5.4 Temperature plot of an ACS intermediate cell for 15% duty factor

the bridge cavity and the ACS end cell is shown in Figure 3.1.2.5.3. The non-symmetrical side coupled cell and the coupling slot of the ACS end cell were redesigned to provide more controllable and stable coupling value, and uniform RF losses distribution in there. As a result, the RF power losses in the bridge cavity are limited inside 4% from the total RF losses of the ACS module. In order to simplify brazing and tuning procedures for mass-production, the side-coupled cell dimensions and outer cell radius in the bridge cavity are fixed for all ACS modules.

The cooling structure of each cavity is based on the design of JHP-ACS with the effective cooling circuit. However, the cooling capacity is improved to realize the good efficiency and uniformity in the operation under large duty factor. Since the partition between accelerating and coupling cells increases in thickness, the cooling channels placement is more convenient. The simulations for temperature distributions, stress analysis and frequency shift estimations were performed with the ANSYS code and the results show that this ACS module can operate with the safe cooling water velocity 2 m/sec under 15% duty factor [9]. That results is shown in Figure 3.1.2.5.4. It ensures the safe module operation for 3% duty factor.

As a result of parameter optimization, the present ACS design has improved in the coupling coefficient and shunt impedance values in comparison with the up-scaled JHP-ACS reference design. The important result is reduction in the outer diameter. It essentially contributes the cost reduction at all stages of the mass-production; material storage, machining, brazing and testing. All changes has been investigated in numerical simulations, discussed and examined for possible sequences. The final experimental proof is now under way with cold models (shown in Figure 3.1.2.5.5).



Figure 3.1.2.5.5. The cells of the half scale 972 MHz ACS cold model.

### References

- [1] V. G. Andreev et al., Proc. of 1972 Proton Linac Conference, (1972) 114.
- [2] Report of the Design Study on the Proton Linac of the JHP [II], KEK Internal 90-16 (1990).
- [3] K. Yamasu et al., Proc. of the 1990 Linac Conference, (1990) 126.
- [4] T. Kageyama et al., Proc. of the 1990 International Linac Conference, (1990) 150.
- [5] Y. Morozumi et al., Proc. of the 1990 International Linac Conference, (1990) 153.
- [6] T. Kageyama et al., Proc. of the 1994 International Linac Conference, (1994) 248.
- [7] JHF Project Office, JHF Accelerator Design Study Report, KEK Report 97-16 (1998).
- [8] V. V. Paramonov, The Annular Coupled Structure optimisation for JAERY/KEK Joint Project for High Intensity Proton Accelerators, KEK Report 2001-14 (2001).
- [9] S. C. Joshi, RF-Thermal - Structural Coupled Analysis of Annuler Coupled Cavity Structure for the Joint Project of KEK/JAERI, KEK-Internal 2001-6 (2001).